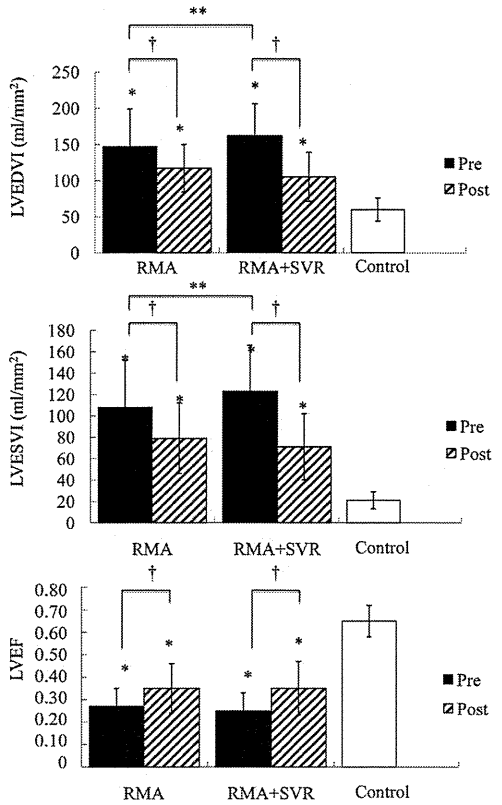

Figure 2. Preoperative (Pre; solid bar) and postoperative (Post; cross-hatched bar) left ventricular volumes and ejection fraction (LVEF) in patients in the restrictive mitral annuloplasty (RMA) and RMA plus surgical ventricular restoration (RMA+SVR) groups and the control group (open bar). †$P<0.05$ between preoperative and postoperative values. *$P<0.05$ vs control. **$P<0.05$ between patients in the RMA and RMA+SVR groups. LVEDVI indicates left ventricular end-diastolic volume index; LVESVI, left ventricular end-systolic volume index.

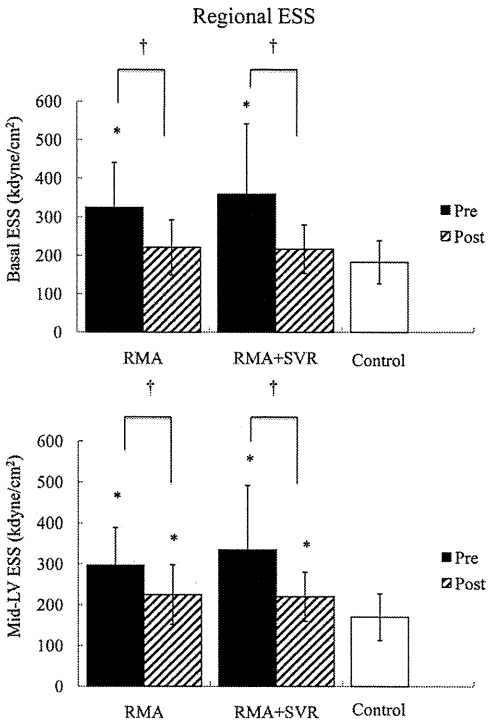

Figure 3. Preoperative (Pre; solid bar) and postoperative (Post; cross-hatched bar) regional end-systolic circumferential myocardial stress (ESS) in the basal and mid-left ventricular (mid-LV) regions in patients in the restrictive mitral annuloplasty (RMA) and RMA plus surgical ventricular restoration (RMA+SVR) groups and the control group (open bar). †$P<0.05$ between preoperative and postoperative values. *$P<0.05$ vs control.

RMA+SVR group than in the RMA group ($P<0.05$ for both), whereas the 2 groups' mean values for postoperative LVEDVI and LVESVI did not differ significantly as of 2.8 months' follow-up ($P>0.05$ for both; Figure 2).

Intraobserver and interobserver agreement for the measurements was assessed with the results from 20 subjects. Good correlation was shown for both the intraobserver (Y. Shudo; LVEDVI $r=0.92$, $P<0.001$; LVESVI $r=0.94$, $P<0.001$; LVEF $r=0.94$, $P<0.001$) and interobserver (Y. Shudo versus K. Takeda; LVEDVI $r=0.93$, $P<0.001$; LVESVI $r=0.95$, $P<0.001$; LVEF $r=0.89$, $P<0.001$) agreement.

Global and Regional Systolic Performance

Global LVEF, which was severely impaired in both study groups preoperatively, showed a significant increase postoperatively ($P<0.001$, respectively; Table 3). Global LVEF in the study groups both preoperatively and postoperatively was significantly lower than in the controls ($P<0.01$, respectively). There was no significant difference between the 2 study groups ($P<0.05$ both preoperatively and postoperatively; Figure 2).

The mean regional CFS in both the basal and mid-LV regions, which was reduced in both study groups preoperatively compared with controls ($P<0.001$, respectively), also increased significantly postoperatively ($P<0.001$, respectively) but was still significantly lower than in the controls ($P<0.01$, respectively). There was no significant difference in either region between the 2 study groups ($P>0.05$ for all).

Regional Circumferential ESS

Preoperatively, regional ESS was markedly elevated in both the basal and mid-LV regions of the LV in both the RMA and RMA+SVR groups compared with the corresponding regions in the controls ($P<0.001$, respectively; Table 3). At the basal region, regional ESS decreased significantly by an average of 142 kdyne/cm^2, from 359 to 217 kdyne/cm^2 (a reduction of 39%) in the RMA+SVR group, and by an average of 98 kdyne/cm^2, from 308 to 210 kdyne/cm^2 (a reduction of 32%) in the RMA group. At the mid-LV region, regional ESS significantly decreased by an average of 115 kdyne/cm^2, from 335 to 220 kdyne/cm^2 (a reduction of 34%) in the RMA+SVR group, and by an average of 60 kdyne/cm^2, from 287 to 227 kdyne/cm^2 (a reduction of 21%) in the RMA group, but the values remained significantly higher for both groups than in the controls ($P<0.01$; Figure 3).

Magnitude of Changes in Global LV Volume, LVEF, and Regional ESS

The percent reductions in LVEDVI and LVESVI were significantly larger in the RMA+SVR group than in the RMA group: $-35\pm20\%$ versus $-21\pm22\%$ for LVEDVI ($P=0.003$) and $-42\pm25\%$ versus $-27\pm28\%$ for LVESVI

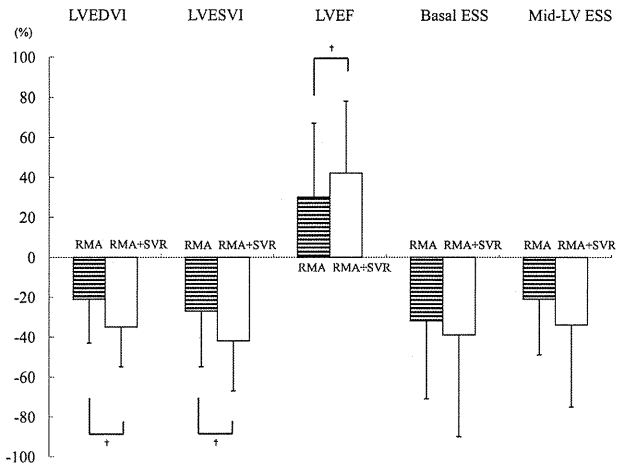

Figure 4. Magnitude of changes in global left ventricular volume, left ventricular ejection fraction (LVEF), and regional end-systolic circumferential myocardial stress (ESS) in the basal and mid-left ventricular (mid-LV) regions in patients in the restrictive mitral annuloplasty (RMA; ▤) and RMA plus surgical ventricular restoration (RMA+SVR; open bar) groups. †$P<0.05$ between RMA group and RMA+SVR group. LVEDVI indicates left ventricular end-diastolic volume index; LVESVI, left ventricular end-systolic volume index.

($P=0.006$). The percent improvement in LVEF was significantly larger in the RMA+SVR group than in the RMA group (42±36% versus 30±37%, $P=0.01$).

The percent reduction of regional ESS in the basal and mid-LV regions tended to be greater in the RMA+SVR group than in the RMA group, although these differences did not reach statistical significance as of 2.8 months after the operation, which reflects the fact that the 2 procedures have different degrees of effects (Figure 4).

Discussion

The major findings of the present study are as follows: (1) LVEDVI and LVESVI were significantly greater in the RMA+SVR group than in the RMA group preoperatively, but they did not differ significantly between the 2 groups postoperatively. (2) LVEDVI and LVESVI decreased significantly, by 21% and 27% after RMA and by 35% and 42% after RMA+SVR, and the percent reductions in LVEDVI and LVESVI were significantly larger in the RMA+SVR group than in the RMA group. (3) Regional ESS and CFS improved significantly in the noninfarcted regions after RMA with or without SVR. The present findings indicated that RMA+SVR had a potentially greater effect in reducing LVEDVI and LVESVI than RMA. Although the role of concomitant SVR at the time of RMA is still controversial and no clear guidelines exist, the present results suggest that selected patients with advanced LV remodeling may benefit from concomitant RMA and SVR. The present data also suggest that regional dysfunction of the residual noninfarcted myocardium is at least partly reversible, although it is unknown whether this reversal is related to the alteration in contractility.

The present study focused on the LV volumetric change, measured by use of MDCT images, associated with RMA with or without SVR in patients with functional MR and ICM. In this small series, the addition of SVR resulted in a significantly greater degree of reduction in LV volume than was achieved with RMA alone. Although this difference might be explained by an additive effect of SVR with RMA, or as a function of the significantly greater preoperative values in this group, it is possible that this effect could contribute to the restoration of anterior/anteroseptal infarcted myocardium. In addition, our results showed that the postoperative LVEDVI and LVESVI were not different between the 2 study groups, which indicates either that SVR does not have a significant effect beyond RMA alone or that SVR is only useful in patients with a more severely dilated LV. However, future studies that control for the preoperative LV volume will be necessary to address this question. Data from a number of studies support the efficacy and use of SVR.[2,7,14,15] Many of these studies have demonstrated that in selected patients with ICM, ventricular reconstruction with various techniques can be accomplished with low operative mortality, improved LV volumes and function, and improved exercise capacity, quality of life, and NYHA class, along with reduced incidents of rehospitalization and good midterm survival.[2,7,14–17]

The recent Surgical Treatment for Ischemic Heart Failure (STICH) trial, which was randomized, concluded that the combination of SVR with CABG results in greater clinical benefits than CABG alone.[4] However, despite the larger reduction in LV end-systolic volume index obtained in their study (19% versus 6%),[4] the findings are strongly debated, largely because the SVR-related volume reductions were much smaller than in other SVR trials (typically 40%).[18] In the present results, the LV end-systolic volume index decreased by 42% (52±31 mL/mm^2) in the SVR+RMA group as of 2.8 months after the operation, which is in line with most previous studies at midterm follow-up, for example, the RESTORE (Reconstructive Endoventricular Surgery returning Torsion Original Radius Elliptical shape to the left ventricle) group (57±34 mL/mm^2),[2] Dor and coworkers (51±18 mL/mm^2),[16] and Di Donate and associates (average of 3 groups: 44±20 mL/mm^2).[17]

The adverse effects of LV dilatation were codified by White and associates,[19] who showed that increased ventricular volume rather than altered ejection fraction became the principal surrogate for mortality, regardless of whether the patient had significant residual coronary artery obstruction. In the present study, even when the LV was severely dilated, our approach (ie, RMA with SVR) was successful, resulting in LV volumetric reduction, wall stress reduction, attenuated LV ejection performance, improved symptoms, and satisfactory early results. These results were similar to those of RMA without SVR in patients with a less dilated LV. These findings may reflect the role of additional SVR as a surrogate for a more severe natural history of increasing morbidity and mortality in dilated hearts, although it is still unknown whether these surgical interventions improve the clinical status of the patient. Therefore, we assume that for selected patients with functional MR who have broad akinesia or dyskinesia associated with relative wall thinning, RMA with SVR is a reasonable surgical option that may prove beneficial.

Previous studies showed that hemodynamic improvement induced by SVR may depend on a complex interplay of changes in LV volume and LV wall stress.[7,8] It is possible that

reverse remodeling may happen in the border zone and induce further improvement in myocardial function.[20] However, chronic changes in myocardial stress, especially in the noninfarcted myocardium, after RMA with or without SVR have not been fully investigated, because it can be difficult to measure regional myocardial stress in LVs with different shapes. In the present study, we attempted to assess the changes in regional myocardial stress after RMA with or without SVR in patients with ICM and functional MR. We observed that regional ESS in the noninfarcted myocardium decreased substantially after RMA with or without SVR. We also observed that regional CFS improved in the same 2 regions after surgery. The present data suggest that regional dysfunction of the residual noninfarcted myocardium may be reversible, at least in part, although whether the improvement is related to the reduction in myocardial wall stress or to an alteration in the myocardial contractile property itself still needs to be evaluated.

Recent advances in steady-state free precession sequencing for cardiac MDCT have resulted in a shorter acquisition time and improved image quality. Considering the relatively short acquisition time and adequate quality of the reconstructed images, 64-row MDCT is a useful clinical tool for assessment of the LV contour in patients with ICM and functional MR.[21] The present study provides an additional approach for evaluation of LV volume, ejection performance, and wall stress, either globally or regionally. Echocardiography has been widely used to measure LV volume in heart failure, but the results are based on geometric assumptions that limit the accuracy of the data. Currently, cardiac magnetic resonance imaging (MRI) is considered the "gold standard" for LV geometry and volume evaluation.[22] It provides excellent temporal and spatial resolution, along with a high degree of accuracy, and reproducible quantitative measurements. Multiphase cine imaging quality is significantly better in MRI than in MDCT because of differences in temporal resolution. However, MRI requires an extended scanning period and cannot be used for patients with a pacemaker. Previous computed tomography studies have shown a good correlation and acceptable agreement of LV volumes and cardiac function compared with MRI.[23,24] This is probably because LV volumes and cardiac function are mainly determined by the end-systolic and end-diastolic phases, when cardiac motion is comparatively minimal and motion artifacts are negligible. Therefore, 64-row MDCT appears to be a useful alternative to 2-dimensional or 3-dimensional echocardiography or MRI in this study population with metal implants (eg, pacemakers or implantable cardioversion-defibrillators), claustrophobia, or other conditions that are not suitable for MRI.

Clinical Implications

On the basis of the present results in patients undergoing RMA who have ICM and functional MR, we favor combining RMA with SVR to exert an additional LV reverse-remodeling effect. In the present study, even when the LV was severely dilated, our approach was successful, and the early results are satisfactory.

Study Limitations

The major limitations of the present study are that it was not conducted in a randomized manner and that it involved a rather small sample size. However, the 100% patient follow-up is a strength. The study would have been stronger with a larger, randomized, and controlled population. In addition, the small sample size could place the study at risk for a type II error. Because we used each patient's preoperative data as his or her baseline, the statistical power was optimized.

Next, the preoperative LV volume differences between the 2 study groups might involve a probable selection bias toward SVR in patients with larger hearts; however, all the patients met the optimal entry criteria, which were the same as in previous studies.[2–5]

Regarding the technical aspects, the variety of surgical procedures and type of annuloplasty ring could have influenced the outcomes. SVR is still not a standardized technique, however, and the optimal procedure remains to be investigated. Concomitant procedures, especially CABG, might have favorably influenced our patients' LV functional improvements. The STICH trial report[4] showed that in 212 patients with LVEF <35% undergoing CABG alone, the mean end-systolic volume index at 4 months after surgery had decreased by an average of 5 mL/m^2, from 82 to 77 mL/m^2 (6% reduction), which indicates that there were no measurable functional improvements in those patients. Moreover, we previously observed no significant improvements in LV volumes, regional stress, or regional CFS in the noninfarcted myocardium at 8 months after CABG alone in patients with severe LV dysfunction.[15] Therefore, we think that the effect of revascularization could be minimized in the present results. Comparison of the fraction of patients who received concomitant CABG in each study group in the present series (RMA versus RMA+SVR; 83% versus 52%) suggests that there was little influence on LV volume, LVEF, or regional stress. However, differences may become obvious with further follow-up, because revascularization effects can be delayed well beyond 3 months in the failing ventricle.[25] We preferably used a semirigid complete annuloplasty ring. A previous report suggests that the type of annuloplasty ring could influence the postoperative LV function[26]; therefore, the present results would not be applicable to patients who received another type of prosthesis. Our results were obtained only from patients who underwent RMA with or without SVR, but the study did not include a control group of patients who did not have either procedure, and withholding surgery from such patients would be unethical in any case. To differentiate between the effects of RMA and SVR, future investigations that include other study groups to compare with patients undergoing SVR to treat functional MR will be required. The patients enrolled in the present study all had ICM associated with anterior or anteroseptal infarction. Therefore, the present results are not applicable to patients with inferior or lateral infarctions or patients with nonischemic dilated cardiomyopathy.

Finally, we used 64-row MDCT as the image modality. As with conventional modalities, MDCT has inherent limitations, including the need for contrast medium and radiation exposure. However, its high spatial resolution enables us to closely estimate regional wall thickness and appropriately compare preoperative values with postoperative values, which makes it particularly useful for estimating regional

myocardial stress. Moreover, given the increased use of cardiac defibrillators or biventricular pacemakers in patients with heart failure, which contraindicate some modalities (eg, MRI), MDCT should prove useful for noninvasively assessing ventricular function, although this point would have been stronger if the results could have been compared with MRI measurements.

Differences in the patients' breath-holding positions between slices and the vertical motion of the mitral annulus can affect the reconstructed images. For this reason, we determined the LV contour by carefully obtaining data from the same plane, as much as possible, before and after surgery. Therefore, differences due to the breath-holding position in the present patient series were negligible, and 3-dimensional reconstruction of the intracardiac anatomy from a series of 2-dimensional images was feasible and clinically useful.

Conclusions

RMA with or without SVR reduced LV end-diastolic and end-systolic volume, which led to improved global ejection performance, reduced regional myocardial wall stress, and improved regional fiber shortening of the noninfarcted myocardium in patients with ICM and functional MR. We found that RMA with SVR reduced the LVEDVI and LVESVI more than RMA alone. In correctly selected patients with more advanced LV remodeling, concomitant SVR may favorably affect the LV reverse-remodeling process induced by RMA.

Acknowledgment

We wish to thank Dr Takashi Daimon, Department of Biostatistics, Hyogo College of Medicine, for his statistical assessment.

Disclosures

None.

References

1. Di Donate M, Sabatier M, Dor V, Toso A, Maioli M, Fantini F. Akinetic versus dyskinetic postinfarction scar: relation to surgical outcome in patients undergoing endoventricular circular patch plasty repair. *J Am Coll Cardiol.* 1997;29:1569–1575.
2. Athanasuleas CL, Buckberg GD, Stanley AW, Siler W, Dor V, Di Donate M, Menicanti L, Almeida de Oliveira S, Beyersdorf F, Kron IL, Suma H, Kouchoukos NT, Moore W, McCarthy PM, Oz MC, Fontan F, Scott ML, Accola KA; RESTORE group. Surgical ventricular restoration in the treatment of congestive heart failure due to post-infarction ventricular dilatation. *J Am Coll Cardiol.* 2004;44:1439–1445.
3. Menicanti L, Castelvecchio S, Ranucci M, Frigiola A, Santambrogio C, de Vincentiis C, Brankovic J, Di Donate M. Surgical therapy for ischemic heart failure: single-center experience with surgical anterior ventricular restoration. *J Thorac Cardiovasc Surg.* 2007;134:433–441.
4. Jones RH, Velazquez EJ, Michler RE, Sopko G, Oh JK, O'Connor CM, Hill JA, Menicanti L, Sadowski Z, Desvigne-Nichens P, Rouleau JL, Lee KL; STITCH Hypothesis 2 Investigators. Coronary bypass surgery with or without surgical ventricular reconstruction. *N Engl J Med.* 2009;23: 360:1705–1717.
5. Maxey TS, Reece TB, Ellman Pl, Butler PD, Kern JA, Tribble CG, Kron IL. Coronary artery bypass with ventricular restoration is superior to coronary artery bypass alone in patients with ischemic cardiomyopathy. *J Thorac Cardiovasc Surg.* 2004;127:428–434.
6. Mehra MR, Reyes P, Benitez RM, Zimrin D, Gammie JS. Surgery for severe mitral regurgitation and left ventricular failure: what do we really know? *J Card Fail.* 2008;14:145–150.
7. Di Donate M, Toso A, Dor V, Sabatier M, Barletta G, Menicanti L, Fantini F; RESTORE Group. Surgical ventricular restoration improves mechanical intraventricular dyssynchrony in ischemic cardiomyopathy. *Circulation.* 2004;109:2536–2543.
8. Tulner SA, Steendijk P, Klautz RJ, Bax JJ, Schalij MJ, van der Wall EE, Dion RA. Surgical ventricular restoration in patients with ischemic dilated cardiomyopathy: evaluation of systolic and diastolic ventricular function, wall stress, dyssynchrony, and mechanical efficiency by pressure-volume loops. *J Thorac Cardiovasc Surg.* 2006;132:610–620.
9. Shudo Y, Matsumiya G, Takeda K, Matsue H, Taniguchi K, Sawa Y. Novel software package for quantifying local circumferential myocardial stress. *Int J Cardiol.* 2011;147:134–136.
10. Dor V, Saab M, Coste P, Kornaszewska M, Montiglio F. Left ventricular aneurysm: a new surgical approach. *Thorac Cardiovasc Surg.* 1989;37: 11–19.
11. Rozich JD, Carabello BA, Usher BW, Kratz JM, Bell AE, Zile MR. Mitral valve replacement with and without chordal preservation in patients with chronic mitral regurgitation: mechanisms for differences in postoperative ejection performance. *Circulation.* 1992;86:1718–1726.
12. Janz RF. Estimation of local myocardial stress. *Am J Physiol.* 1982;242: H875–H881.
13. Grigioni F, Enriquez-Sarano M, Zehr KJ, Bailey KR, Tajik AJ. Ischemic mitral regurgitation: long-term outcome and prognostic implications with quantitative Doppler assessment. *Circulation.* 2001;103:1759–1764.
14. Mickleborough LL, Merchant N, Ivanov Joan, Carson S. Left ventricular reconstruction: early and late results. *J Thorac Cardiovasc Surg.* 2003; 128:27–36.
15. Taniguchi K, Sakurai M, Takahashi T, Imagawa H, Mitsuno M, Nakano S, Kawashima Y, Matsuda H. Postinfarction left-ventricular aneurysm: regional stress, function, and remodeling after aneurysmectomy. *Thorac Cardiovasc Surg.* 1998;46:253–259.
16. Dor V, Civaia F, Alexandrescu C, Montiglio F. The post-myocardial infarction scarred ventricle and congestive heart failure: the preeminence of magnetic resonance imaging for preoperative, intraoperative, and postoperative assessment. *J Thorac Cardiovasc Surg.* 2008;136:1405–1412.
17. Di Donate M, Castelvecchio S, Kukulski T, Bussadori C, Giacomazzi F, Frigiola A, Menicanti L. Surgical ventricular restoration: left ventricular shape influence on cardiac function, clinical status, and survival. *Ann Thorac Surg.* 2009;87:455–461.
18. Buckberg GD, Athanasuleas CL. The STICH trial: misguided conclusions. *J Thorac Cardiovasc Surg.* 2009;138:1060–1064.
19. White HD, Norris RM, Brown MA, Brandt PW, Whitlock RM, Wild CJ. Left ventricular end-systolic volume as the major determinant of survival after recovery from myocardial infarction. *Circulation.* 1987;76:44–51.
20. Yu HY, Chen YS, Tseng WY, Chi NS, Wang CH, Wang SS, Lin FY. Why is the surgical ventricular restoration operation effective for ischemic cardiomyopathy? Geometric analysis with magnetic resonance imaging of changes in regional ventricular function after surgical ventricular restoration. *J Thorac Cardiovasc Surg.* 2009;137:887–894.
21. Bellenger NG, Burgess MI, Ray SG, Lahiri A, Coats AJ, Cleland JG, Pennell DJ. Comparison of left ventricular ejection fraction and volumes in heart failure by echocardiography, radionuclide ventriculography and cardiovascular magnetic resonance: are they interchangeable? *Eur Heart J.* 2000;21:1387–1396.
22. Kaji S, Nasu M, Yamamuro A, Tanabe K, Nagai K, Tani T, Tamita K, Shiratori K, Kinoshita M, Senda M, Okada Y, Morioka S. Annular geometry in patients with chronic ischemic mitral regurgitation: three-dimensional magnetic resonance imaging study. *Circulation.* 2005; 112(suppl):I-409–I-414.
23. Reman SV, Shar M, McCarthy B, Garcia A, Ferketich AK. Multi-detector row cardiac computed tomography accurately quantifies right and left ventricular size and function compared with cardiac magnetic resonance. *Am Heart J.* 2006;151:736–744.
24. Wu YW, Tadamura E, Yamamuro M, Kanao S, Okayama S, Ozasa N, Toma M, Kimura T, Komeda M, Togashi K. Estimation of global and regional cardiac function using 64-slice computed tomography: a comparison study with echocardiography, gated-SPECT and cardiovascular magnetic resonance. *Int J Cardiol.* 2008;128:69–76.
25. Bondarenko O, Beek AM, Twisk JW, Visser CA, van Rossum AC. Time course of functional recovery after revascularization of hibernating myocardium: a contrast-enhanced cardiovascular magnetic resonance imaging. *Eur Heart J.* 2008;29:200–205.
26. David TE, Komeda M, Pollick C, Burns RJ. Mitral valve annuloplasty: the effect of the type on left ventricular function. *Ann Thorac Surg.* 1989;47:524–528.

Circulation
JOURNAL OF THE AMERICAN HEART ASSOCIATION

American Heart Association®
Learn and Live℠

Induced Adipocyte Cell-Sheet Ameliorates Cardiac Dysfunction in a Mouse Myocardial Infarction Model : A Novel Drug Delivery System for Heart Failure

Yukiko Imanishi, Shigeru Miyagawa, Norikazu Maeda, Satsuki Fukushima, Satoru Kitagawa-Sakakida, Takashi Daimon, Ayumu Hirata, Tatsuya Shimizu, Teruo Okano, Iichiro Shimomura and Yoshiki Sawa

Circulation 2011, 124:S10-S17
doi: 10.1161/CIRCULATIONAHA.110.009993
Circulation is published by the American Heart Association. 7272 Greenville Avenue, Dallas, TX 72514
 Print ISSN: 0009-7322. Online ISSN: 1524-4539

Induced Adipocyte Cell-Sheet Ameliorates Cardiac Dysfunction in a Mouse Myocardial Infarction Model

A Novel Drug Delivery System for Heart Failure

Yukiko Imanishi, PhD; Shigeru Miyagawa, MD, PhD; Norikazu Maeda, MD, PhD; Satsuki Fukushima, MD, PhD; Satoru Kitagawa-Sakakida, MD, PhD; Takashi Daimon, PhD; Ayumu Hirata, MD, PhD; Tatsuya Shimizu, MD, PhD; Teruo Okano, PhD; Iichiro Shimomura, MD, PhD; Yoshiki Sawa, MD, PhD

Background—A drug delivery system that constitutively and effectively retains cardioprotective reagents in the targeted myocardium has long been sought to treat acute myocardial infarction. We hypothesized that a scaffold-free induced adipocyte cell-sheet (iACS), transplanted on the surface of the heart, might intramyocardially secrete multiple cardioprotective factors including adiponectin (APN), consequently attenuating functional deterioration after acute myocardial infarction.

Methods and Results—Induced ACS were generated from adipose tissue–derived cells of wild-type (WT) mice (C57BL/6J), which secreted abundant APN, hepatocyte growth factor, and vascular endothelial growth factor in vitro. Transplanted iACS secreted APN into the myocardium of APN-knockout (KO) mice at 4 weeks. APN was also detected in the plasma of iACS-transplanted APN-KO mice at 3 months (245±113 pg/mL). After left anterior descending artery ligation, iACS, generated from either WT (n=40) or APN-KO (n=40) mice, were grafted onto the surface of the anterior left ventricular wall of WT mice, or only left anterior descending artery ligation was performed (n=43). Two days later, inflammation and infarct size were significantly diminished only in the WT-iACS treated mice. One month later, cardiomyocyte diameter and percent fibrosis were smaller, whereas ejection fraction and survival were greater in the WT-iACS treated mice compared with the KO-iACS–treated or nontreated mice.

Conclusions—Cardioprotective factors including APN, hepatocyte growth factor, and vascular endothelial growth factor were secreted from iACS. Transplantation of iACS onto the acute myocardial infarction heart attenuated infarct size, inflammation, and left ventricular remodeling, mediated by intramyocardially secreted APN in a constitutive manner. This method might be a novel drug delivery system to treat heart disease. (***Circulation.* 2011;124[suppl 1]:S10–S17.**)

Key Words: acute myocardial infarction ■ adiponectin ■ cell therapy ■ drug delivery system ■ tissue engineering

Despite recent progress in medical and surgical treatments for heart failure, acute myocardial infarction (AMI) and the subsequent deterioration of cardiac performance is still a major cause of death, worldwide. An array of cardioprotective reagents have been identified to be effective in ameliorating AMI by administrating into the infarcted myocardium in experimental models.[1] However, these reagents have failed to show consistent therapeutic efficacy in several clinical trials, probably due to poor retention or rapid inactivation of reagents in the injured myocardial tissues.[1] Therefore, a drug delivery system (DDS) that retains cardioprotective reagents in the targeted myocardial area has long been sought.

Intramyocardially transplanted autologous stem cells secrete various cardioprotective cytokines and growth factors, enhance angiogenesis, reduce fibrosis, attenuate apoptosis, and suppress myocyte hypertrophy, consequently ameliorating AMI in a paracrine manner.[2,3] However, cell transplantation for AMI has shown only modest therapeutic efficacy in large-scale clinical studies. It appears to result from insufficient paracrine effects whose magnitude and figure are largely affected by the cell delivery method or transplanted cell source.[4] To enhance the survival and functions of the transplanted cells, we developed a cell-sheet–based delivery method in which isolated cells, cultivated in vitro as a sheet without a scaffold, are simply placed on the surface of the myocardium. This treatment enhances the paracrine effects, resulting in better therapeutic efficacy.[5,6]

Adipocytes differentiated from adipose tissue–derived stromal-vascular fraction (SVF) cells are a promising cell

From the Department of Cardiovascular Surgery (Y.I., S.M., S.F., S.K.-S., Y.S.) and the Department of Metabolic Medicine (N.M., A.H., I.S.), Graduate School of Medicine, Osaka University, Suita, Osaka, Japan; the Division of Biostatistics (T.D.), Department of Mathematics, Hyogo College of Medicine, Nishinomiya, Hyogo, Japan; and the Institute of Advanced Biomedical Engineering and Science (T.S., T.O.), Tokyo Women's Medical University, Shinjuku-ku, Tokyo, Japan.

Presented at the 2010 American Heart Association meeting in Chicago, IL, November 12–16, 2010.

The online-only Data Supplement is available at http://circ.ahajournals.org/lookup/suppl/doi:10.1161/CIRCULATIONAHA.110.009993/-/DC1.

Correspondence to Yoshiki Sawa, 2-2 Yamada-oka, Suita City, Osaka 565-0871, Japan. E-mail sawa@surg1.med.osaka-u.ac.jp

Circulation **is available at http://circ.ahajournals.org** **DOI: 10.1161/CIRCULATIONAHA.110.009993**

source for treating AMI because as they secrete hepatocyte growth factor (HGF), vascular endothelial growth factor (VEGF), and, importantly, adiponectin (APN).[7,8] APN is a circulating secretory protein that has multiple cardioprotective effects, including the attenuation of inflammation, fibrosis, and myocyte hypertrophy.[8,9] However, the clinical use of APN for treating AMI has been hampered by the lack of effective systems for delivering APN to the heart. We hypothesized that using cell-sheet technology to deliver adipocytes that secrete multiple cardioprotective factors, including APN, might attenuate the functional deterioration after AMI.

Methods

Animal care complied with the "Guide for the Care and Use of Laboratory Animals" (NIH publication No. 85 to 23, revised 1996). Experimental protocols were approved by the Ethics Review Committee for Animal Experimentation of Osaka University Graduate School of Medicine.

Generation and Assessment of Adipocyte Cell-Sheet

The SVF cells of adipose tissue were isolated from wild-type (WT; male C57BL/6J) or APN-knockout (KO) mice,[10] as described previously.[11] The isolated SVF cells were cultured until they become confluent on Upcell dishes (CellSeed Inc, Tokyo, Japan). Differentiation into adipocytes was induced by insulin, dexamethasone, isobutylmethylxanthine, and pioglitazone (Sigma-Aldrich, MO). Incubation at 20°C induced the cells to detach from the culture dishes, yielding a scaffold-free cell-sheet, which we call an "induced adipocyte cell-sheet" (iACS). The secretion of HGF, VEGF, leptin, interleukin (IL)-6, tumor necrosis factor (TNF)-α, and IL-10 into the culture supernatant was assessed by ELISA. Before transplantation, WT mouse–derived iACS (WT-iACS) and APN-KO mouse–derived iACS (KO-iACS) were labeled with the use of a PKH26 kit (Sigma-Aldrich).

Generation of AMI Model and Cell-Sheet Transplantation

An AMI model was generated by permanent ligation of the left anterior descending artery (LAD) in male C57BL/6J mice, 10 to 15 weeks old.[12] The mice were anesthetized by isoflurane inhalation (Mylan Inc). Five minutes after the LAD ligation, WT-iACS (W group, n=40) or KO-iACS (K group, n=40) was grafted onto the surface of the anterior left ventricular (LV) wall, or a sham operation was performed (C group, n=43). The mice were euthanized at 2 and 28 days after LAD ligation and cell-sheet transplantation.

Assessment of Cardiac Function and Survival

Cardiac function was assessed with the use of an echocardiography system equipped with a 12-MHz transducer (GE Healthcare) at 4 weeks. The LV dimensions were measured, and LV ejection fraction was calculated as $(LVDd^3-LVDs^3)/LVDd^3\times100$, where LVDd and LVDs are the LV end-diastolic and end-systolic dimensions, respectively.[12] The mice were housed in a temperature-controlled incubator for 50 days after treatment to determine their survival.

Histological Analysis

Freshly excised hearts were stained with 1% 2,3,5-triphenyltetrazolium chloride (TTC; Sigma-Aldrich). The red-stained infarct area was quantified by computerized planimetry, using MetaMorph Software (Molecular Devices). Frozen sections (8 μm) of hearts and cell-sheets were stained with antibodies against APN (Otsuka Pharmaceutical, Tokushima, Japan) or CD11b (Abcam, Cambridge, UK). The secondary antibody was Alexa 488 goat anti-rabbit (Life Technologies). Counterstaining was performed with 6-diamidino-2-phenylindole (Life Technologies). To analyze the myocardial collagen accumulation, heart sections were stained with Masson trichrome. The collagen volume fraction was calculated in the peri-infarct area. To assess cardiomyocyte diameter, heart sections were stained with periodic acid-Schiff. MetaMorph Software was used for the quantitative morphometric analysis.

Cytokine Antibody Array

Proteins were isolated from whole-heart samples and analyzed using a Milliplex Mouse Cytokine/Chemokine Panel Premixed 32Plex, according to the manufacturer's instructions (Millipore).

Quantitative Real-Time PCR

Total RNA was isolated from the peri-infarct area by use of the RNeasy Mini Kit and reverse-transcribed, using Omniscript Reverse transcriptase (Qiagen, Hilden, Germany). Quantitative PCR was performed with the PCR System (Life Technologies). The expression of each mRNA was normalized to that of glyceraldehyde-3-phosphate dehydrogenase.

Statistical Analysis

Data are expressed as the mean±SEM. The data distributions were checked for normality with the Shapiro-Wilk test and for equality of variances with the Bartlett test. Comparisons between 2 groups were made using the unpaired t test or the Wilcoxon-Mann-Whitney U test, as appropriate. For comparisons among 3 groups, we used 1-way ANOVA, followed by Fisher protected least-significance difference test or the Kruskal-Wallis test, followed by the post hoc pairwise Wilcoxon-Mann-Whitney U test, as appropriate. The survival curves were prepared by using the Kaplan-Meier method and were compared using the overall log-rank test, followed by the post hoc pairwise log-rank test. The multiplicity in pairwise comparisons was corrected by the Benjamin-Hochberg procedure. All probability values are 2-sided, and values of $P<0.05$ were considered to indicate statistical significance. Statistical analysis was performed with the StatView 5.0 Program (Abacus Concepts, Berkeley, CA) and the R program.[13]

An expanded Methods section can be found in the online-only Data Supplement.

Results

Characterization of the Adipocyte Cell-Sheets

Most SVF cells differentiated into mature adipocytes bearing oil droplets by 7 days after differentiation induction. Induced ACS or undifferentiated SVF cell-sheets were then generated by lowering the temperature (Figure 1A). Each iACS was approximately 7 mm in diameter (Figure 1B) and 100 μm thick (Figure 1C). WT-iACS expressed abundant APN in the cytoplasm and extracellular matrix around the oil-droplet–rich adipocytes, as assessed by immunohistochemistry (Figure 1D) and ELISA (Figure 1E). In contrast, neither the SVF cell-sheets of either origin nor the KO-iACS expressed APN (Figure 1D and 1E). The ELISA showed abundant HGF expression in WT-iACS and KO-iACS, which was downregulated compared with the WT SVF cells (Figure 1F). The secretion of VEGF and leptin was remarkably enhanced by the SVF cell differentiation into adipocytes. IL-6 and IL-10 were secreted by the WT-iACS and WT-SVF cells at similar levels, which were lower than the levels secreted by KO-iACS. The secretion of TNF-α was not evident in any group because the cell-free culture medium also contained 2.29 pg/mL TNF-α.

Transplanted Induced ACS Supplied APN to the Myocardium

WT-iACS were transplanted onto the heart of intact APN-KO mice to evaluate behavior of the WT-iACS, including APN

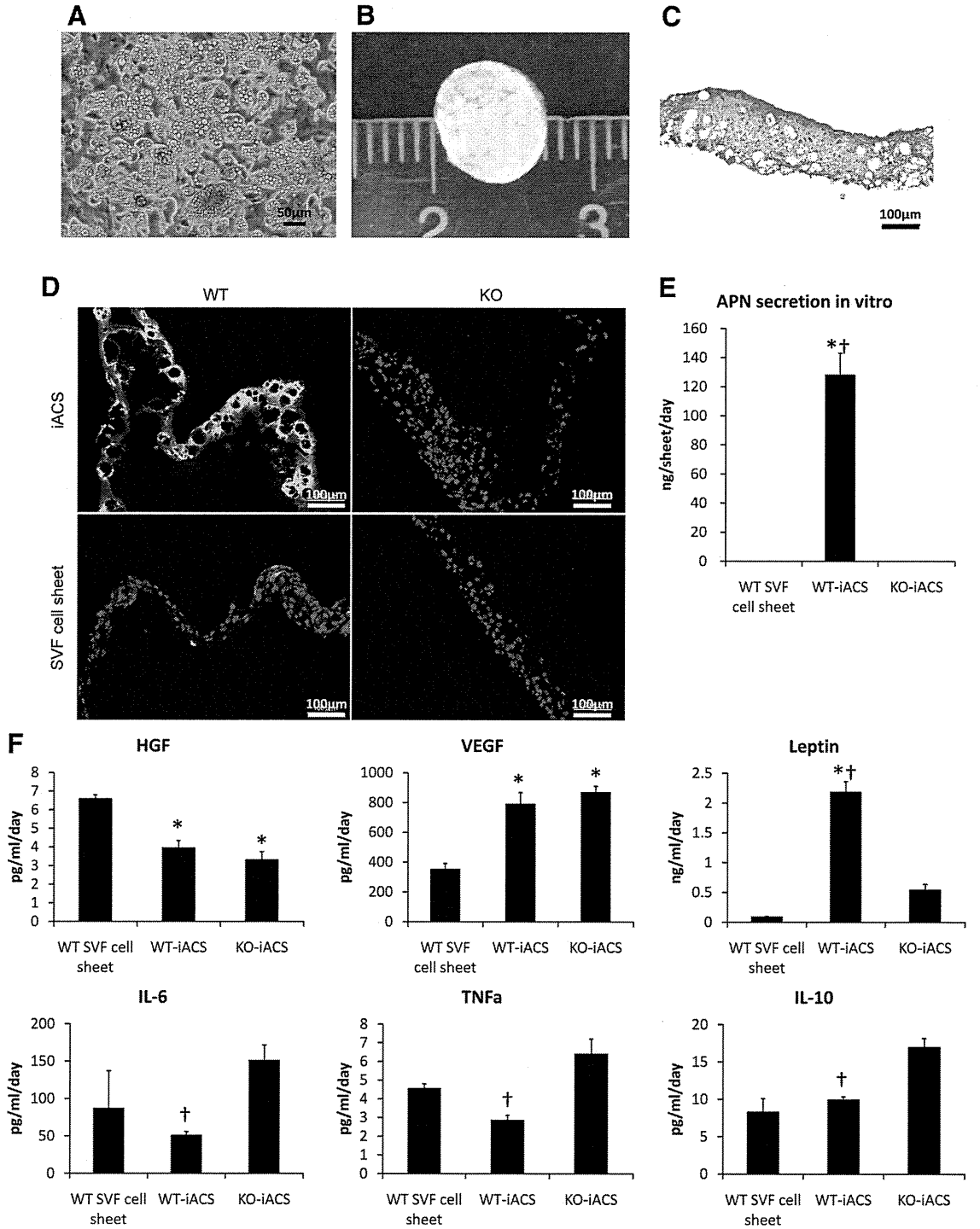

Figure 1. Characterization of induced adipocyte cell-sheet (iACS) in vitro. **A**, Histological analysis showing mature adipocytes with oil droplets in the cytosol. **B**, Induced ACS detached from the temperature-responsive culture dish. **C**, Cross-sectional view of hematoxylin and eosin–stained iACS. **D**, Representative pictures of adiponectin (APN)-stained cell-sheets. Wild-type (WT)-iACS showed strong labeling for APN. The WT stromal-vascular fraction (SVF) cell-sheet, knockout (KO)-iACS, and KO SVF cell-sheet were negative for APN. Green indicates APN; blue, nuclei. **E**, APN secretion into the WT-iACS culture supernatant determined by ELISA (WT SVF cell sheet, n=2; WT-iACS, n=5; KO-iACS, n=8; $P<0.05$, Kruskal-Wallis test). *$P<0.05$ versus WT SVF cell-sheet, †$P<0.05$ versus KO-iACS, post hoc Wilcoxon-Mann-Whitney *U* test. **F**, Hepatocyte growth factor (HGF), vascular endothelial growth factor (VEGF), leptin, interleukin (IL)-6, IL-10, and tumor necrosis factor (TNF)-α secretion into the culture supernatant, measured by ELISA. WT-iACS secreted HGF, VEGF, leptin, IL-6, and IL-10 but not TNF-α (WT SVF cell sheet, n=2; WT-iACS, n=8 to 12; KO-iACS, n=6 to 9). HGF, VEGF, and leptin ($P<0.05$, ANOVA); *$P<0.05$ versus WT SVF cell-sheet, †$P<0.05$ versus KO-iACS, post hoc Fisher protected least-significance difference test. TNF-α, IL-6, and IL-10 ($P<0.05$, Kruskal-Wallis test); *$P<0.05$ versus WT SVF cell-sheet, †$P<0.05$ versus KO-iACS, post hoc Wilcoxon-Mann-Whitney *U* test.

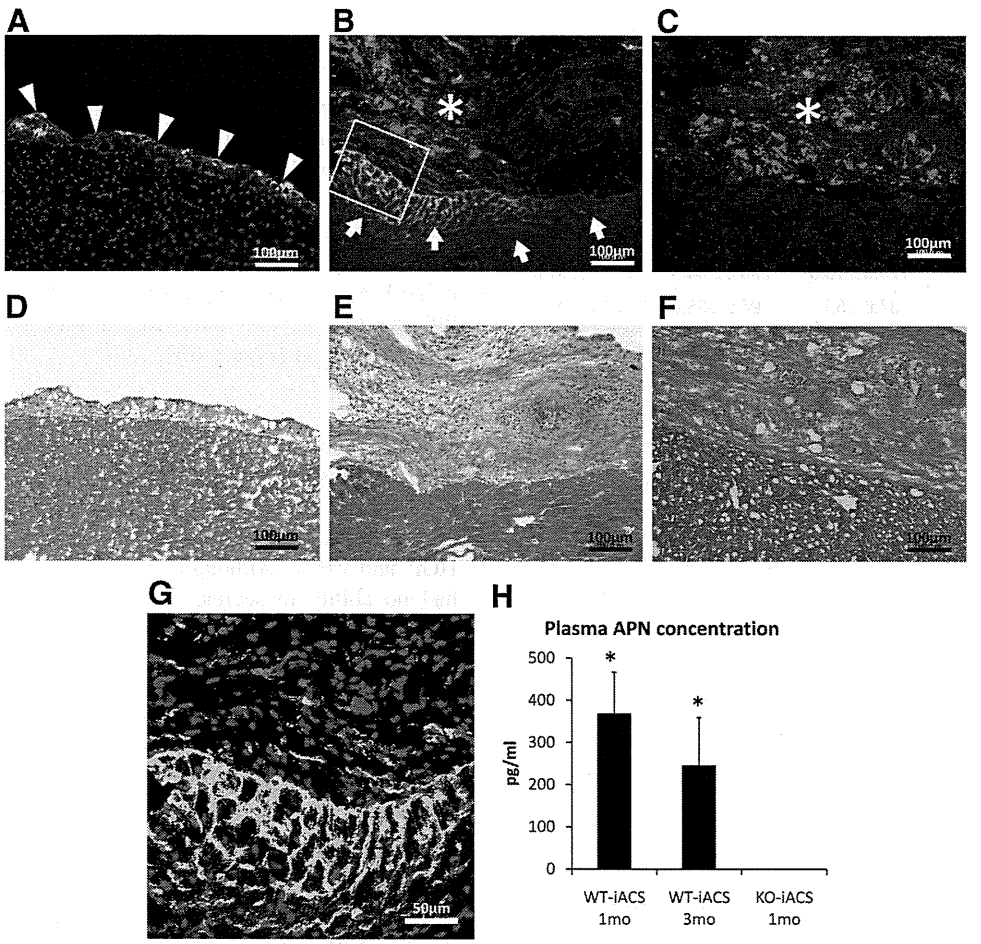

Figure 2. Local and systemic delivery of induced adipocyte cell-sheet (iACS)-derived adiponectin (APN) in vivo. **A**, Immediately after wild-type (WT)-iACS implantation onto the knockout (KO) mouse heart, iACS-expressed APN was detected on the epicardium. Arrowheads show the implanted WT-iACS. Green indicates APN; blue, nuclei. **B**, WT-iACS stained with red fluorescent dye were implanted onto KO myocardium. Twenty-eight days after transplantation, APN was detected both in the surviving WT-iACS and the extracellular matrix (ECM) of the KO mouse myocardium at the implanted site. Asterisk indicates the implanted WT-iACS. Arrows show iACS-derived APN in the host myocardium. **C**, KO-iACS stained with red fluorescent dye and implanted onto KO myocardium. Twenty-eight days after transplantation, the implanted KO-iACS survived, but no APN was detected in the KO-iACS or the ECM. Asterisk indicates the implanted KO-iACS. Green indicates APN; red, KO-iACS; and blue, nuclei. **D** through **F**, Hematoxylin and eosin staining of a serial section from the sample in **A**, **B**, and **C**, respectively. **G**, High-magnification image of the square in **B** and **H**. Plasma APN concentration of WT-iACS (WT) or KO-iACS (KO) recipient APN-KO mice. APN was detected in the WT group plasma 1 (n=4) and 3 months (n=3) after transplantation but not in the KO group plasma (n=4, $P<0.05$, Kruskal-Wallis test). *$P<0.05$ versus KO 1 month, post hoc Wilcoxon-Mann-Whitney *U* test.

production. Immediately after transplantation, the WT-iACS expressed APN epicardially at the anterior LV wall, but it was not expressed intramyocardially (Figure 2A). Four weeks after transplantation, the WT-iACS had survived, was approximately 600 μm thick, and contained adipocytes and connective tissue. At this time, the WT-iACS was tightly integrated with the epicardium, but no invasion of transplanted cells into the recipient myocardium was observed (Figure 2B and 2E). APN was expressed in the cytoplasm of scattered surviving WT-iACS cells and in the myocardium close to the WT-iACS (Figure 2B and 2G). In contrast, although the KO-iACS transplanted into KO mice survived (Figure 2C and 2F), they did not express or secrete APN (Figure 2C). When WT-iACS was transplanted into KO mice, APN was detected in the plasma 1 and 3 months later, but it was not detected in the plasma of KO mice with the KO-iACS implant (Figure 2H).

Induced ACS Implantation Reduced Inflammatory Responses and Infarct Area 2 Days After MI

The anti-inflammatory effects of WT-iACS were evaluated by cytokine antibody array analysis of whole-heart lysates from the AMI mice that were treated with WT-iACS (W), KO-iACS (K), or no iACS (C) groups at 2 days after implantation (Table). A significantly lower level of the inflammatory factor granulocyte macrophage colony-stimulating factor (GM-CSF) was observed in the W group compared with the others, and the levels of other inflammatory cytokines, keratinocyte chemoattractant, IL-6, granulocyte (G)-CSF, and monocyte chemotactic protein-1 (MCP-1) showed a trend toward downregulation in the W group. Quantitative RT-PCR showed that the TNFα mRNA levels were lower in the peri-infarct area of the W group than in that of the K and C groups, which reached statistical significance in the W group (Figure 3A). Furthermore, immunohistochem-

Table. Cytokine Antibody Array

	W Group (n=4)	K Group (n=5)	C Group (n=6)
Granulocyte macrophage colony-stimulating factor, pg	0.0±0*†	21.8±1.3	18.5±6.7
Keratinocyte chemoattractant, pg	292.7±42.7	539.9±56.4	629.9±113.1
Interleukin-6, pg	175.3±16.0	295.3±44.0	281.4±51.5
Granulocyte-colony stimulating factor, pg	37.6±5.7	94.6±35.0	52.8±9.5
Monocyte chemotactic protein-1, pg	316.4±51.9	467.6±50.4	388.7±87.1

$P<0.05$, Kruskal-Wallis test.
*$P<0.05$ versus C group.
†$P<0.05$ versus K group, post hoc Wilcoxon-Mann-Whitney U test.

istry for CD11b showed significantly fewer infiltrated macrophages in the peri-infarct area of the W and K groups than in that of the C group (Figure 3B). Finally, a semiquantitative assessment by TTC staining showed that the infarct area was significantly smaller in the W group than in the K and C groups (Figure 4).

Induced ACS Transplantation Suppressed LV Remodeling Development at 4 Weeks After MI

Four weeks after LAD ligation, the C group showed a typical MI with a large anterior LV scar, dilatation of the LV cavity, and cardiomyocyte hypertrophy. By comparison, the LV of the W group was less dilated, and the anterior wall was thicker (Figure 5A). The diameter of the cardiomyocytes was significantly smaller in the W group (Figure 5B and 5C), and there was less collagen accumulation (Figure 5D and 5E). There was no difference in capillary density among the groups (online-only Data Supplement Figure 1).

Therapeutic Effects of Induced ACS Transplantation on Cardiac Performance and Survival at 4 Weeks After MI

Cardiac performance was evaluated by 2D echocardiography 4 weeks after implantation. Both the diastolic and systolic LV dimensions were smaller in the W group than the others, but the difference was not significant. In contrast, LV ejection fraction was significantly greater in the W group than the K and C groups (Figure 6A). In addition, in a WT-iACS–transplanted rat model of acute MI, invasive hemodynamic analysis showed higher end-systolic pulmonary vascular resistance and dP/dtmax and lower dP/dtmin, compared with sham transplantation (online-only Data Supplement Figure 2). Mortality was substantial until 14 days after LAD ligation in the K and C groups. In contrast, in the W group, there was little mortality 5 days after MI and thus a significant difference in survival (Figure 6B).

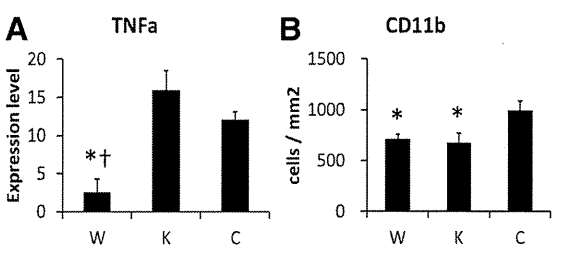

Figure 3. Induced adipocyte cell-sheet (iACS) effects on inflammatory responses after myocardial infarction at the implant/myocardium border zone 2 days after implantation. **A**, Quantitative RT-PCR results for the tumor necrosis factor (TNF)-α transcript. TNF-α transcription was significantly lower in the W group (n=4) than in the K (n=4) and C groups (n=6, $P<0.05$, Kruskal-Wallis test) *$P<0.05$ versus C group, †$P<0.05$ versus K group, post hoc Wilcoxon-Mann-Whitney U test. **B**, Quantification of CD11b-positive cells. The number of CD11b-positive cells was significantly lower in the W (n=4) and K (n=4) groups than in the C group (n=6, $P<0.05$, ANOVA). *$P<0.05$ versus C group, Fisher protected least-significance difference test.

Discussion

We developed an adipocyte cell-sheet–based DDS for the heart. These sheets, which are generated from adipose tissue–derived SVF cells induced to differentiate in culture, secreted multiple cardioprotective factors in vitro, including APN, HGF, and VEGF. Although adipose tissue–derived SVF cells had no ability to secrete APN, after the differentiation to adipocytes, the cells started to secrete APN in addition to HGF and VEGF. APN was secreted from the iACS into the myocardium and blood for at least 3 months, probably along with HGF, VEGF, leptin, and IL-10. In a mouse model of AMI, WT-iACS significantly decreased inflammation and myocardial infarct size at the acute stage. Furthermore, myocardial fibrosis and cardiomyocyte hypertrophy were significantly attenuated at the late stage, which led to improved cardiac performance and a better post-MI survival rate. Importantly, the transplantation of KO-iACS onto infarcted hearts resulted in only modest therapeutic benefits, indicating that APN plays a pivotal role in attenuating the AMI in this experimental model.

There have been many experimental and clinical studies in which the administration of exogenous proteins, including APN, induced angiogenesis, reversed remodeling, and improved cardiac function.[1,14] The issues in this method may be that naked protein is delivered to the heart and is often poorly retained or quickly inactivated and therefore lacks long-term efficacy.[15] MI is a progressive disease, characterized by massive ischemic necrosis of the myocardial tissue and subsequent inflammation. This leads to cardiac remodeling that exacerbates the oxygen shortage in the surviving cardiac tissue. These pathological and functional deteriorations eventually cause end-stage heart failure. A constitutive and balanced supply of cardioprotective reagents, rather than the 1-time administration of a single reagent, should inhibit this vicious circle. The direct injection of plasmid vectors encoding targeted reagents and the transplantation of genetically modified cells can provide a controlled and stable supply of reagents over the long term; however, their clinical use is limited because the safety of the viral systems used as vectors for the plasmids and of modifying cells for transplant is still a concern.[16] Encapsulation as the DDS for biomaterials is another attractive approach; however, difficulty in controlling the rate of reagent release, such as the occurrence of an initial burst release, limits its therapeutic efficacy.[17,18] In addition, biodegradable polymers that carry reagents may induce the deposition of extracellular matrix and myocardial inflamma-

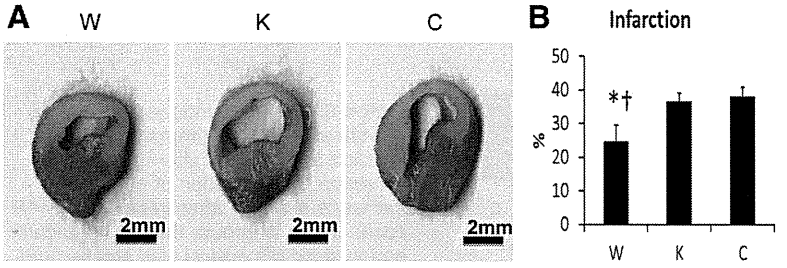

Figure 4. Infarct area of induced adipocyte cell-sheet (iACS)-treated heart 2 days after myocardial infarction. **A**, Representative 2,3,5-triphenyltetrazolium chloride staining images at border zone of infarct. **B**, Quantification of infarct size. The percent infarcted area was significantly lower in the W group (n=8) compared with the other groups (K, n=7; C, n=9; $P<0.05$, ANOVA). *$P<0.05$ versus C group. †$P<0.05$ versus K group, Fisher protected least-significance difference test.

tion, leading to pathological fibrotic states.[19] Our cell-sheet–based DDS constitutively and effectively delivered multiple cardioprotective factors over the long term, leading to reverse LV remodeling after MI, without gene modification or scaffold use. Thus, this strategy might be more practical and effective than other methods for delivering therapeutic proteins for treating MI in the clinical arena.

It is possible that the delivery of multiple growth factors will improve therapeutic efficacy over the delivery of a single factor. This hypothesis is supported by a study showing that the combination of HGF and VEGF leads to better engraftment and significant angiogenesis, compared with either factor alone.[20] In our study, the KO-iACS, which secreted HGF and VEGF but not APN, reduced macrophage infiltration but did not induce functional or survival benefits. These benefits were conferred by the WT-iACS, which produced APN, suggesting that APN's benefits are different from and in addition to those of known paracrine mediators, such as HGF or VEGF.

APN is a protective factor against cardiovascular diseases.[9,21] In particular, its anti-inflammatory properties may be the major reason for its beneficial effects on cardiovascular disorders, because APN-deficient mice exhibit increased TNF-α production and myocardial apoptosis in response to ischemia reperfusion.[22,23] We observed that the expression of TNF-α in the AMI heart was significantly reduced by transplanting WT-iACS but not KO-iACS, which secrete similar levels of the same cytokines, except for APN, suggesting that the direct anti-inflammatory effects of APN played a key role in the attenuated inflammation in this study. In addition, the infarct size was significantly smaller in the WT-iACS–transplanted hearts than in the KO-iACS–transplanted ones. Infarct size is determined by multiple factors, including the magnitude of ischemic stimuli, degree of

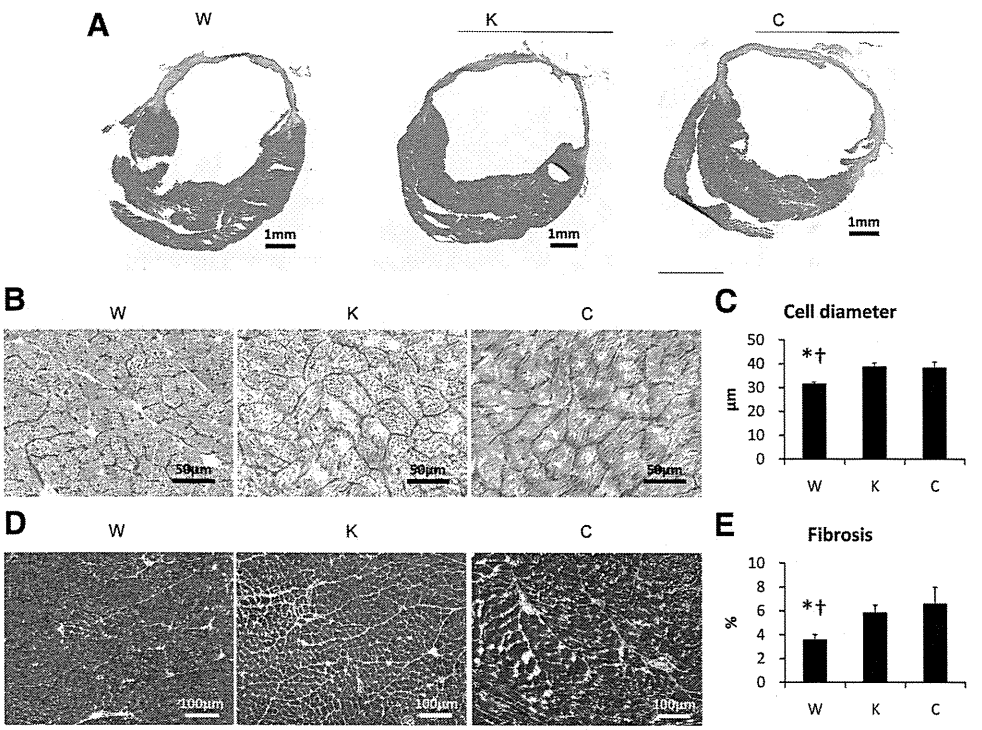

Figure 5. Effects on left ventricular remodeling by induced adipocyte cell-sheet (iACS) transplantation 4 weeks after myocardial infarction. **A**, Representative macro images from each group. **B**, Representative periodic acid-Schiff staining of tissue remote from infarct site. **C**, Quantification of cardiomyocyte diameter. Cardiomyocyte diameters in the tissue remote from the infarct site were significantly smaller in the W group (n=6) than in the other groups (K, n=8; C, n=5; $P<0.05$, ANOVA). *$P<0.05$ versus C group. †$P<0.05$ versus K group, Fisher protected least-significance difference test. **D**, Representative Masson trichrome staining images at the border area. **E**, Quantification of percent fibrosis. Fibrosis at the border area was significantly suppressed in the W group (n=6) compared with the other groups (K, n=8; C, n=5; $P<0.05$, Kruskal-Wallis test). *$P<0.05$ versus C group. †$P<0.05$ versus K group, post hoc Wilcoxon-Mann-Whitney *U* test.

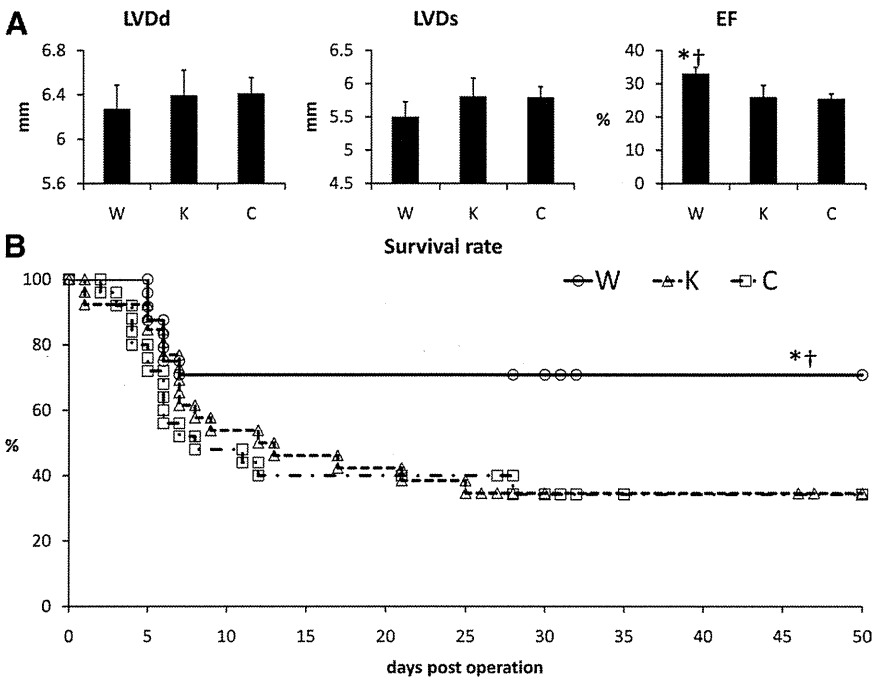

Figure 6. Wild-type induced adipocyte cell-sheet (WT-iACS) improved cardiac function and survival after myocardial infarction. **A**, Evaluation of cardiac performance 4 weeks after treatment (n=18 each). In the W group, the left ventricular end-systolic dimension was smaller and the ejection fraction significantly higher than in the other groups ($P<0.05$, Kruskal-Wallis test). *$P<0.05$ versus C group. †$P<0.05$ versus K group, post hoc Wilcoxon-Mann-Whitney *U* test. **B**, Survival rates after treatment. There was no significant difference between the C (n=25) and K groups (n=26). The W group (n=24) showed significantly better survival than the other groups ($P<0.05$, overall log-rank test). *$P<0.05$ versus C group, †$P<0.05$ versus K group, post hoc log-rank test.

inflammation, and amount of apoptosis. The beneficial effects of APN on inflammation after the iACS treatment may have led to the attenuated infarct size and suppressed the exacerbation of cardiac performance. In addition, APN has been shown to directly inhibit the hypertrophic response in myocytes.[24] Therefore, the combined direct and indirect actions of APN probably inhibit the development of pathological hypertrophy and preserve myocardial mass. Although we traced the iACS-derived APN by using APN-KO mice to demonstrate the APN delivery, HGF, VEGF, and other beneficial growth factors are probably also released constitutively by the iACS. Thus, iACS can provide a combined and balanced release of multiple paracrine mediators that may synergistically augment therapeutic benefits.[20,23]

On the other hand, APN is reported to have proangiogenic potential.[9] In fact, VEGF secretion from WT-iACS and KO-iACS were also greater compared with undifferentiated WT-SVF cell-sheet in this study. However, the capillary density in the treated myocardium, which was assessed by CD31 immunohistolabeling, was not higher at 28 days after WT-iACS transplantation, compared with post–KO-iACS transplantation and sham transplantation. These inconsistent findings may result from the AMI model in which neoangiogenesis substantially occurs in the treated area, not allowing dissection of the slight difference in capillary density between the experimental groups. Rather, the findings of this study suggested that anti-inflammatory effects were the major mechanism for the improvement after WT-iACS transplantation in this model. Another disease model such as dilated cardiomyopathy and old myocardial infarction may be more appropriate to evaluate angiogenic property of iACS treatment.

The treatment strategy for AMI studied here is not directly applicable to the clinical arena, because the time required to isolate, cultivate, or manipulate cells in vitro is not available for AMI, which requires immediate treatment. However, the finding that this therapy yielded marked cardioprotective effects through constitutive APN production should be beneficial for treating other types of cardiac pathologies, such as the chronic phase of MI, dilated cardiomyopathy, or myocarditis. In addition, this sophisticated cell-sheet, which elevates the systemic APN level for some time, might also be effective for treating systemic disorders such as obesity-linked cardiovascular or metabolic disorders, although this possibility will require further investigation.[9,21]

A potential limitation of this study is that the small sample sizes in our experiments limit their statistical power. Thus, the apparent absence of a statistical difference may be due to the lack of statistical power to detect small differences; therefore our negative results may have no meaning. Nevertheless, despite the small sample sizes, we at least clearly showed that APN was delivered by WT-iACS and that the therapeutic effect of WT-iACS implantation was attained through APN. Furthermore, we conducted multiple statistical tests for significance separately for each outcome in a univariate manner, although we adjusted for multiple pairwise testing between groups within each outcome. Such tests for multiple outcomes could lead to the inflation of the type I error probability in making treatment effect claims.

In the present study, we focused on the delivery of cytokines by iACS. However, we speculate that other mechanisms may also contribute to the functional recovery after iACS implantation. Tateno et al[25] clearly showed that cell transplantation induces the recipient tissue to produce angiogenic factors, including IL-1β, even though the transplanted cells do not produce sufficient levels of cytokines to promote angiogenesis directly. Similarly, iACS may stimulate recipient tissue, thus activating cells in the recipient to produce angiogenic cytokines. Further study will be required to elucidate what cross-talk occurs between the iACS and the recipient myocardium.

In summary, iACS may be a powerful DDS for cytokines, including APN, HGF, and VEGF. The implantation of iACS onto the infarcted mouse heart reduces the infarct size, inflammation, and LV remodeling. This method is probably adaptable as a novel DDS for treating heart failure.

Acknowledgments

We thank Masako Yokoyama and Yoko Motomura for excellent technical assistance.

Sources of Funding

This study was funded in part by a grant-in-aid for Scientific Research (22659251) from the Ministry of Education, Culture, Sports, Science, and Technology of Japan.

Disclosures

Dr Shimizu is a consultant for CellSeed, Inc. Dr Okano is an Advisory Board Member in CellSeed, Inc, and an inventor/developer designated on the patent for temperature-responsive culture surfaces.

References

1. Hwang H, Kloner RA. Improving regenerating potential of the heart after myocardial infarction: factor-based approach. *Life Sci.* 2010;86:461–472.
2. Vandervelde S, van Luyn MJ, Tio RA, Harmsen MC. Signaling factors in stem cell-mediated repair of infarcted myocardium. *J Mol Cell Cardiol.* 2005;39:363–376.
3. Gnecchi M, Zhang Z, Ni A, Dzau VJ. Paracrine mechanisms in adult stem cell signaling and therapy. *Circ Res.* 2008;103:1204–1219.
4. Herrmann JL, Abarbanell AM, Weil BR, Wang Y, Wang M, Tan J, Meldrum DR. Cell-based therapy for ischemic heart disease: a clinical update. *Ann Thorac Surg.* 2009;88:1714–1722.
5. Miyagawa S, Saito A, Sakaguchi T, Yoshikawa Y, Yamauchi T, Imanishi Y, Kawaguchi N, Teramoto N, Matsuura N, Iida H, Shimizu T, Okano T, Sawa Y. Impaired myocardium regeneration with skeletal cell sheets–a preclinical trial for tissue-engineered regeneration therapy. *Transplantation.* 2010;90: 364–372.
6. Shimizu T, Sekine H, Yamato M, Okano T. Cell sheet-based myocardial tissue engineering: new hope for damaged heart rescue. *Curr Pharm Design.* 2009;15:2807–2814.
7. Nakagami H, Morishita R, Maeda K, Kikuchi Y, Ogihara T, Kaneda Y. Adipose tissue-derived stromal cells as a novel option for regenerative cell therapy. *J Atheroscler Thromb.* 2006;13:77–81.
8. Maeda K, Okubo K, Shimomura I, Funahashi T, Matsuzawa Y, Matsubara K. CDNA cloning and expression of a novel adipose specific collagen-like factor, apm1 (adipose most abundant gene transcript 1). *Biochem Biophys Res Commun.* 1996;221:286–289.
9. Shibata R, Ouchi N, Murohara T. Adiponectin and cardiovascular disease. *Circ J.* 2009;73:608–614.
10. Maeda N, Shimomura I, Kishida K, Nishizawa H, Matsuda M, Nagaretani H, Furuyama N, Kondo H, Takahashi M, Arita Y, Komuro R, Ouchi N, Kihara S, Tochino Y, Okutomi K, Horie M, Takeda S, Aoyama T, Funahashi T, Matsuzawa Y. Diet-induced insulin resistance in mice lacking adiponectin/acrp30. *Nat Med.* 2002;8:731–737.
11. Planat-Benard V, Silvestre JS, Cousin B, Andre M, Nibbelink M, Tamarat R, Clergue M, Manneville C, Saillan-Barreau C, Duriez M, Tedgui A, Levy B, Penicaud L, Casteilla L. Plasticity of human adipose lineage cells toward endothelial cells: physiological and therapeutic perspectives. *Circulation.* 2004;109:656–663.
12. Imanishi Y, Saito A, Komoda H, Kitagawa-Sakakida S, Miyagawa S, Kondoh H, Ichikawa H, Sawa Y. Allogenic mesenchymal stem cell transplantation has a therapeutic effect in acute myocardial infarction in rats. *J Mol Cell Cardiol.* 2008;44:662–671.
13. R Development Core Team. R: A language and environment for statistical computing. 2008. R Foundation for Statistical Computing; Vienna, Austria. ISBN 3-900051-07-0. http://www.R-project.org. Accessed August 3, 2011.
14. Kondo K, Shibata R, Unno K, Shimano M, Ishii M, Kito T, Shintani S, Walsh K, Ouchi N, Murohara T. Impact of a single intracoronary administration of adiponectin on myocardial ischemia/reperfusion injury in a pig model. *Circ Cardiovasc Interv.* 2010;3:166–173.
15. Davis ME, Hsieh PC, Grodzinsky AJ, Lee RT. Custom design of the cardiac microenvironment with biomaterials. *Circ Res.* 2005;97:8–15.
16. Yla-Herttuala S, Martin JF. Cardiovascular gene therapy. *Lancet.* 2000; 355:213–222.
17. Joung YK, Bae JW, Park KD. Controlled release of heparin-binding growth factors using heparin-containing particulate systems for tissue regeneration. *Expert Opin Drug Deliv.* 2008;5:1173–1184.
18. Allison SD. Analysis of initial burst in PLGA microparticles. *Expert Opin Drug Deliv.* 2008;5:615–628.
19. Xia Z, Triffitt JT. A review on macrophage responses to biomaterials. *Biomed Mater.* 2006;1:R1–R9.
20. Golocheikine A, Tiriveedhi V, Angaswamy N, Benshoff N, Sabarinathan R, Mohanakumar T. Cooperative signaling for angiogenesis and neovascularization by VEGF and HGF following islet transplantation. *Transplantation.* 2010;90:725–731.
21. Hopkins TA, Ouchi N, Shibata R, Walsh K. Adiponectin actions in the cardiovascular system. *Cardiovasc Res.* 2007;74:11–18.
22. Ouchi N, Walsh K. Adiponectin as an anti-inflammatory factor. *Clin Chim Acta.* 2007;380:24–30.
23. Shibata R, Sato K, Pimentel DR, Takemura Y, Kihara S, Ohashi K, Funahashi T, Ouchi N, Walsh K. Adiponectin protects against myocardial ischemia-reperfusion injury through AMPK- and COX-2-dependent mechanisms. *Nat Med.* 2005;11:1096–1103.
24. Shibata R, Ouchi N, Ito M, Kihara S, Shiojima I, Pimentel DR, Kumada M, Sato K, Schiekofer S, Ohashi K, Funahashi T, Colucci WS, Walsh K. Adiponectin-mediated modulation of hypertrophic signals in the heart. *Nat Med.* 2004;10:1384–1389.
25. Tateno K, Minamino T, Toko H, Akazawa H, Shimizu N, Takeda S, Kunieda T, Miyauchi H, Oyama T, Takeda S, Kunieda T, Miyauchi H, Oyama T, Matsuura K, Nishi J-i, Kobayashi Y, Nagai T, Kuwabara Y, Iwakura Y, Nomura F, Saito Y, Komuro I. Critical roles of muscle-secreted angiogenic factors in therapeutic neovascularization. *Circ Res.* 2006;98:1194.

SUPPLEMENTAL MATERIALS

MS ID#: CIRCULATIONAHA/2010/009993/R1

MS TITLE: Induced Adipocyte Cell-Sheet Ameliorates Cardiac Dysfunction in Mouse Myocardial Infarction Model - A Novel Drug Delivery System for Heart Failure

Materials and Methods

Preparation of Adipocyte cell-sheet

Stromal-vascular fraction (SVF) cells were enzymatically isolated from adipose tissues.[1] Briefly, inguinal adipose tissue was excised from wild type mice (WT; male C57BL/6J), APN knockout (KO) mice which were generated and backcrossed to C57BL/6J over 6 generations as described previously[2], or from rats (3-week-old, male LEW/Sea). Adipose tissue was digested in Hank's balanced buffered saline (Sigma-Aldrich, MO, USA) containing 0.1% collagenase type II (Life Technologies, CA, USA) at 37°C with shaking vigorously for 1 hour. The adipose cell extracts were passed 100 μm and 70 μm filters, resuspended in Dulbecco's Modified Eagle's Medium (Life Technologies) containing 10% fetal bovine serum (Equitech-bio, TX, USA), 200 μM ascorbic acid (Sigma-Aldrich), and antibiotics (Life Technologies), then cultured on culture dishes (AGC Techno Glass, Chiba, Japan) at 37°C and 5% CO_2. Twenty-four hours after plating, all the non-adherent cells were removed by washing. The SVF cells were cultured for 3 days in

the same medium. The SVF cells were then seeded at 7000 cells/cm^2 in an Upcell dish, which is coated with temperature-responsive polymers (CellSeed, Tokyo, Japan). The culture area was 1.9 cm^2 for mouse cells and 8.8 cm^2 for rat cells. Seven days after passage, the SVF cells were induced to differentiate into the adipogenic lineage by adding 0.87 μM insulin, 0.25 μM dexamethasone, 500 μM isobutylmethylxanthine (IBMX), and 5 μM Pioglitazone (Sigma-Aldrich) for 48 hours. Seven days after induction, the adipocytes were induced to spontaneously detach by placing the plates at 20 °C for 1 hour, yielding a scaffold-free sheet-shaped monolayer of induced adipocyte cell-sheet (iACS) that could be used as a graft. Finally, two iACS were layered to make a thicker sheet for grafting. Both WT mouse-derived iACS and APN-KO mouse-derived iACS were either assessed *in vitro* or labeled using a PKH26 red fluorescent linker kit (Sigma-Aldrich) prior to transplantation.

Enzyme-Linked Immunosorbent Assay

To determine the content of the secreted factors, enzyme-linked immunosorbent assays (ELISA) were performed. The collected culture supernatant of the WT-iACS, WT SVC cell-sheet or KO-iACS was centrifuged to remove debris and contaminating cells. For APN, samples were diluted 1:200 and analyzed (W, n=5; K, n=8). APN content of plasma samples from iACS-received APN-KO mice were analyzed with no dilutions (W 1 mo, n=4; W 3 mo, n=3; K

1 mo, n=4). An APN ELISA kit was purchased from Otsuka Pharmaceutical (Tokushima, Japan) according to the manufacturer's instructions. Content of HGF, VEGF, leptin, IL-6, IL-10, and TNFα in the culture supernatants were also analyzed by ELISA kit (R&D systems, MN, USA) with no dilutions (W, n=8-12; K, n=6-9).

Animal experiments

Myocardial infarction (MI) model of mice was created by left anterior descending artery (LAD) ligation as described previously.[3] Mice (10-15-weeks old, male C57BL/6J) were anesthetized by inhalation of isoflurane (1.5%, 1L/min, Mylan Inc., Pittsburgh, PA) provided by an anesthetic gas machine (DS Pharma, Osaka, Japan). The anesthetized mice were intubated in an endotracheal manner, and positive pressure ventilation was maintained with a ventilator (room air, 90 cycles/minutes, tidal volume 1 ml, Shinano, Tokyo, Japan). Then, the heart was exposed through a left lateral thoracotomy. With minimal manipulation of the fat pad surrounding the heart, the LAD component could easily be visualized. LAD was ligated with an 8-0 prolene suture (Johnson & Johnson, NJ, USA) at 1 mm distal to the left atrial appendage, immediately after bifurcation of the major left coronary artery. The myocardial ischemic area was visually assessed, to confirm that the LAD ligation had consistent ischemic effects. Procedure-related mortality, which occurred prior to chest closure, was consistently 6% in all the experimental

groups, suggesting a consistent level of acute myocardial ischemia. Within 5 minutes after LAD ligation, the mice were randomly allocated into 3 groups; those that underwent transplantation of WT-iACS (W group; n=40), those that underwent transplantation of KO-iACS (K group; n=40) and those that underwent sham transplantation (C group; n=43). The pericardium was closed to prevent the dislocation of iACS. The mice were allowed to recover under care. In the experiment of iACS implantation to APN-KO mice, MI was not induced.

The mice were euthanized at 2 and 28 days after surgery by intravenous injection of pentobarbital (200 mg/kg body weight; DS Pharma) and 30 mM of potassium chloride (Wako Pure Chemical Industries, Osaka, Japan) to cause cardiac arrest in diastole under terminal anesthesia, and the heart was excised.

On day 2, the specimens for RNA analyses were cut transversely, and then the apex-side specimens were dissected to remove the right ventricular free wall, and part in the three pieces of infarction, peri-infarction, and remote, and soaked in RNA Later (Qiagen, Hilden, Germany, W, n=4; K, n=4; C, n=6). The specimens for CD11b staining were cut into 4 segments, embedded in OCT compound (Sakura Finetek Japan, Tokyo, Japan), and snap frozen in liquid nitrogen (W, n=4; K, n=4; C, n=6). The appropriate segments used for gene expression or histological analyses on day 2 were also used for TTC staining (W, n=8; K, n=7; C, n=9). The specimens used for the cytokine-array analysis were snap frozen in liquid nitrogen on day 2 (W,

n=4; K, n=5; C, n=6). The remaining mice were used for survival-rate analysis (W, n=24; K, n=26; C, n=25), but cases of accidental death were excluded. Twenty-eight days after treatment, 18 mice from each group were randomly chosen for cardiac performance analysis by echocardiography. Histological analyses were also performed at 28 days (W, n=6; K, n=8; C, n=5).

MI was also created in rats (8-week-old, female LEW/Sea) by the same method described above, except the tidal volume was 4 ml. Five minutes after LAD ligation, either two layers of iACS were transplanted onto the LV (n=9) or a sham transplantation was performed (n=6). Four weeks after the operation, a hemodynamic assessment was performed.

Quantitative real time PCR

Total RNA was isolated from the stored specimens using the RNeasy Mini Kit (Qiagen) and reverse transcribed with Ominiscript Reverse transcriptase (Qiagen). Quantitative PCR was performed with the ABI 7500 Fast Real-Time PCR System (Life Technologies) using Taqman Universal Master Mix (Life Technologies). Measurement copy number of mRNA was performed in triplicate. The primers and probes are shown in the Table. All probes were designed with a 5' fluorogenic probe 6FAM and a 3' quencher TAMURA. The results were normalized to glyceraldehyde-3-phosphate dehydrogenase (GAPDH).

Determination of infarct size

Freshly excised hearts from the W, K, and C groups 2 days after transplantation were washed in PBS and dissected into four transverse slices. The slices were then stained for 5 min at 37°C with 1% 2,3,5-triphenyltetrrazolium chloride (TTC; Sigma-Aldrich) to determine the infarct area. The stained slices were photographed, and then the infarct area was determined by computerized planimetry using MetaMorph Software (Molecular Device, CA, USA).

Histological analysis

Histological analyses of the hearts were performed 2 and 28 days after transplantation. The hearts and cell-sheets were cut into 8-μm sections. The sections were stained with antibodies for APN (1:1000 dilution; Otsuka Pharama), CD11b (1:100 dilution; Abcam, Cambridge, UK), or CD31 (1:200 dilution; Abcam). The secondary antibody was Alexa 488 goat anti-rabbit (1 μg/ml; Life Technologies). Counterstaining was with 6-diamidino-2-phenylindole (DAPI; 1 μg/ml; Life Technologies). Images were captured by fluorescence microscopy (Keyence, Osaka, Japan). Routine hematoxylin-eosin staining was performed. Masson's trichrome staining was performed to analyze the collagen accumulation. The collagen volume fraction in the peri-infarct area was calculated as the percentage of the myocardium. The data were collected

from 10 individual views per heart at a magnification of ×200. Furthermore, the heart sections were stained with Periodic acid-Schiff (PAS) to assess the cardiomyocyte size. Cardiomyocyte size at a magnification of ×400 was average from 50 myocytes per sample. MetaMorph Software was used for quantitative morphometric analysis.

Myocardial echocardiography

Echocardiography examinations were performed 4 weeks after cell transplantation by an investigator blinded to the group identities (n=18 each). Two-dimensional, targeted M-mode tracings were obtained at the level of the papillary muscles with an echocardiography system equipped with a 12-MHz transducer (GE Healthcare, WI, USA). The left ventricular (LV) dimensions were measured following the method of the American Society of Echocardiology from at least 3 consecutive cardiac cycles. Three readings were obtained from each mouse and averaged. The LV ejection fraction (EF) was calculated as $(LVDd^3\text{-}LVDs^3)/LVDd^3\times100$, where LVDd is the LV end-diastolic dimension and LVDs is the LV end-systolic dimension.[4]

Hemodynamic analysis

Four weeks after LAD ligation and cell-sheet transplantation, rats (iACS-treated group, n=9; sham-treated group, n=6) were anesthetized and ventilated. A silk thread was placed under the